Abstract: New mining processes are moving toward driverless, autonomous vehicles, however, these will require the ability to detect and avoid large fragments which may block crusher activities. A detection system that can penetrate the surface of the rock pile and determine the presence of over-sized fragments could assist the system in avoiding large fragments. This paper presents the results of experiments with Ground Penetrating Radar (GPR) showing it is possible to use centroid frequency downshift to determine bulk density of the media as an indicator of fragment size. This research is based on an underground mine currently under construction.

Author Address: abenter@csu.edu.au/ mantolovich@csu.edu.au

Determining Bulk Density Of Mine Rock Piles Using Ground Penetrating Radar Frequency Downshift

Allen Benter, Michael Antolovich, Wayne Moore
Centre for Research into Complex Systems
Charles Sturt University
Bathurst, Australia
abenter@csu.edu.au

***Abstract*—New mining processes are moving toward driverless, autonomous vehicles, however, these will require the ability to detect and avoid large fragments which may block crusher activities. A detection system that can penetrate the surface of the rock pile and determine the presence of over-sized fragments could assist the system in avoiding large fragments. This paper presents the results of experiments with Ground Penetrating Radar (GPR) showing it is possible to use centroid frequency downshift to determine bulk density of the media as an indicator of fragment size. This research is based on an underground mine currently under construction.**

I. Introduction

The need to determine the size of fragments before crushing is present in all mines employing secondary breakage. In a typical underground mining scenario, the Load Haul Dump (LHD) vehicle (see Fig. 1 (centre)) collects ore fragments from the draw point (See Fig. 2). Initially the ore that presents at the draw point may be interspersed with large fragments which may, or may not, be visible. Presently the driver of the LHD would visually inspect the draw point to observe any large fragments at the surface. Fragments partially or totally obscured beneath the surface, which remain undetected, present a potential blockage to the crusher unit, preventing subsequent loads from being processed. If a large fragment is present, the draw point is closed and a secondary breakage crew would manually break the fragment into smaller fragments.

The current research is focused on a new underground mine at Cadia (near Orange, NSW, Australia) using the block caving method (see Fig. 3) where the rock breaks up as it collapses toward the extraction point. The ore body caves in from above, gradually falling toward the draw points. As it tumbles, the rock is crushed together, resulting in smaller fragments until they present at the draw point. While over time the incidence of large rocks presenting is expected to reduce, the early stages of extraction are likely to suffer from the appearance of over sized fragments requiring secondary breakage. Detecting these fragments at an early stage will allow the planned closure of draw points, and prevent over sized fragments from entering the crusher.

Figure 1. Remote tele-operation (left) of Sandvik LHD mining vehicle (centre) using vehicle mounted cameras (right) (Source: Sandvik AB)

As stated above, current practices allow for the driver of the LHD to monitor the draw point for over sized fragments. However, new mining processes are moving towards driverless, semi-autonomous vehicles. These are controlled remotely using tele-operation with optical cameras (see Fig. 1 (left and right)) providing the remote driver with 2D vision of the draw point. The authors are researching sensors and processing methods to augment the image provided to the remote operator, assisting with detection of over sized fragments whether partially or wholly beneath the surface. This research will also assist the implementation of fully autonomous vehicles in the underground mine [1] by providing automated large fragment detection.

For efficient processing we need to know if a large fragment is present before the load enters the crusher unit. Ideally this would occur at the draw point (see Fig. 2), before the LHD has collected the ore, allowing the fragment to remain at the draw point for the secondary breakage crew. Automatic detection of fragment sizes using optical cameras has been researched at the draw point, during collection (in the LHD bucket) and after crushing [3]. Optical imaging in underground mines suffers from many extrinsic problems (dust, poor lighting, vibration) in imaging the surface of the rock pile. Techniques to determine fragment sizes have, thus, relied upon the large fragment being visible at the surface of the rock pile. However, this is not always the case.

In order to detect large fragments beneath the surface, a penetrative sensor is required. GPR has been used for observing

Figure 2. A typical draw point in the underground mine. Large rocks which can block primary crushers may be hidden beneath the surface.

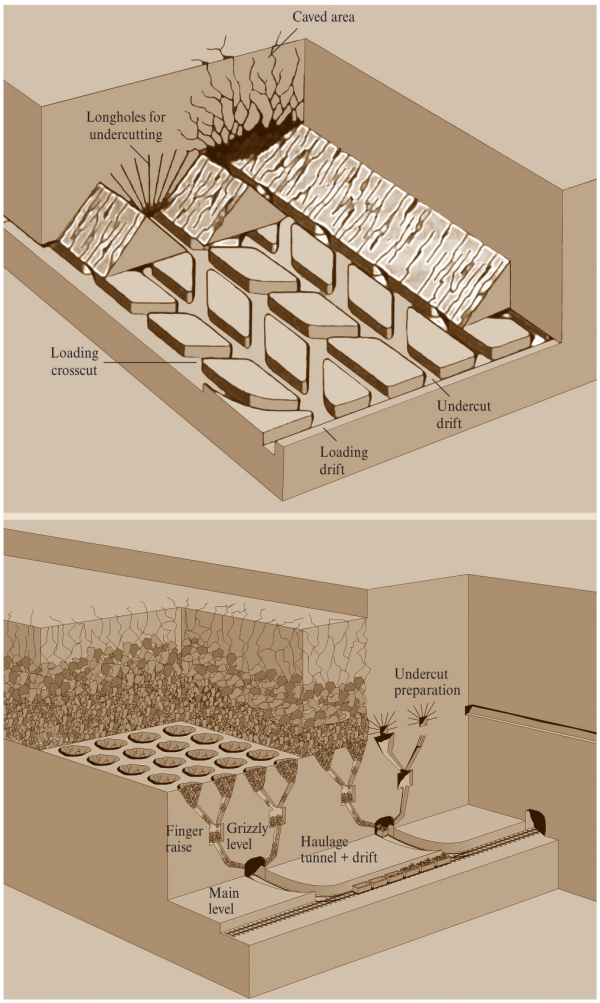

Figure 3. Exploded view of a block cave mine. (Source [2])

features beneath the surface of the earth for archaeology [4], mapping underground voids [5] and non-destructive testing of concrete structures [6]. In most cases, the subject has electromagnetic characteristics distinct from the material in which it is embedded, a particular example being locating land mines [7].

The underground mining operation which is the subject for this research project, features an ore body which is tunnelled for access and then fractured for collection. The large fragments which are the subject of our GPR image exhibit the same electromagnetic characteristics as the ore material surrounding them. In a highly fractured zone featuring small fragments, there are air pockets surrounding the fragments. These present a different electromagnetic signature to the ore, representing a means of detecting fragment sizes through the detection of the air-ore interface. Put another way, where large fragments exist there are no air pockets, and the GPR image will show a homogeneous material response.

In order to improve the detection of large fragments, the resolution of the GPR unit could be improved, thus providing greater discrimination of fragment outlines to enable determination of particle sizes. The Authors have been developing and refining algorithms to enhance the resolution of GPR rock pile images [8]. Higher frequency imaging could provide the improved resolution, however this would also limit the depth of penetration of the signal. This work is continuing independent of, but complementary to, the research presented in this paper.

The depth of penetration required in the underground mine scenario is around 2m, representing the extent of the collection zone for the LHD. The ore, like other earth materials, acts as a low pass filter, removing high frequency components necessary for fine resolution imaging. Hence, an alternative method of investigation is sought to complement the direct imaging of the fragment.

The fragmented nature of the ore changes the homogeneous nature of the rock into a mixture of ore and air pockets, thereby changing the dielectric characteristics of the material dependent on the bulk density of the ore bodies. Examining the medium to determine density, and thus infer the size of particles in the zone of illumination, has already been investigated in road pavement density testing [9]. Reference [10] use GPR to determine the presence of failures in sub-road structures.

A detection system that could penetrate the surface of the fragment pile and determine the presence of over sized fragments could assist remote operators in avoiding large fragments. The following sections will describe experimental results of signal attenuation to determine the bulk density of material under illumination by a GPR signal. Section II will discuss the centroid frequency downshift method. Section III will describe the characteristics of the ore samples; Section IV will present the results of the experiments using GPR,

concluding with Section IV.

II. Centroid Frequency Downshift

Measuring signal amplitude attenuation characteristics as a means of identifying features beneath the surface has been investigated for road pavement substrate failure analysis [10], road pavement density analysis [9] and railroad ballast fouling detection [11]. While [12] looks to correct the attenuation to improve resolution, it is possible to use the attenuation to determine characteristics of the ore.

Typically the time domain is used to prepare two-dimensional (B-scan) and/or three-dimensional (C-scan) images for analysis. The frequency domain has been used to determine the electrical characteristics of soil [13] and concrete [6].

As the GPR pulse propagates into the ore material, it suffers attenuation as a result of absorption, dispersion, scattering and spreading. The propagating wave is subject to three constitutive dielectric characteristics of the medium - complex dielectric permittivity (ϵ), magnetic permeability (μ) and electrical conductivity (σ)). Magnetic permeability is negligible in non-ferrous minerals.

The attenuation, α, of the GPR signal in many geological materials is approximated by a linear function of frequency by:

$$\alpha = \omega \left[\frac{\mu\epsilon}{2} \left(\sqrt{1 + \tan^2 \delta} - 1 \right) \right]^{\frac{1}{2}}$$

where

$$\tan \delta = \frac{\sigma}{\omega\epsilon}$$

and $\omega = 2\pi f$ is the angular frequency; μ = magnetic permeability, in henries per meter; ϵ = dielectric permittivity, in farads per metre; σ = electrical conductivity, in Siemens per metre; f = frequency, in hertz. Hence, higher frequencies attenuate more than low frequencies [14].

Changes in bulk density for rocks will change the dielectric properties of the rock, μ, ϵ and σ, attenuating the transmitted radar signals. The spectrum centroid of the radar pulse experiences a downshift during propagation which can be attributed to dielectric losses [15]. This method of estimation needs the frequency data to be broadband making it easier to detect a change in the frequency distribution.

Losses through scattering are dependent on a number of factors including the frequency, the size of the particles and shape of the object. As the wavelength approaches the size of the particles, the degree of scattering will increase [16]. In order to determine the wavelength, through the material, the velocity of the signal through the samples was calculated through two-way travel time as

$$v = \frac{2d}{t}$$

which allows us to calculate the relative permittivity according to

$$v = \frac{c}{\sqrt{\epsilon_r}}$$

and the wavelength of the signal as

$$\lambda = \frac{v}{f}$$

where v is the velocity in m/s; d is the distance to the aluminium plate beneath the sample boxes; t is the time recorded in the trace to the aluminium plate; $c = 3 \times 10^8 m/s$; ϵ_r is the relative dielectric permittivity; λ is the wavelength in m; and f is the frequency of the propagating wave in the ore in hertz.

The CFDS technique has been applied to detecting attenuation characteristics between two subsurface layers [17]. In the current research, if different attenuation properties can be detected in varying fragmented rock concentrations the estimate can be drawn as to the presence or absence of a whole rock or rubble.

III. Sample Ore Characteristics

The Authors are investigating rock piles from a porphyry copper deposit bearing approximately 1 g/t gold and 0.38% copper. After fracturing using a block caving method, the ore is presented at the draw point for collection, with sizes ranging from small (< 25 mm) to very large (> $1m^3$). It is these very large fragments that the Authors are interested in detecting.

Approximately 20 tonnes of ore samples were obtained from the mine. This was hand sifted and sorted by a 100mm sieve, then a 50mm sieve, followed by a 25mm sieve, with those fragments passing each sieve being retained for the experiments. Fragments larger than 100mm have been excluded from this set of experiments. All visible contaminants were removed (concrete, fibre reinforcing, metal etc) to ensure uniform material.

The experiments were carried out in our laboratory using samples sifted to uniform sizes and contained in plastic boxes of dimensions 600mm x 400mm x 270mm (length x width x depth). For each fragment sample size (<25mm, 25-50mm, 50-100mm) three boxes were filled by pouring the rock samples into the boxes to a depth of between 220mm and 250mm. These boxes were stacked 3 high to achieve a maximum sample depth with an aluminium plate beneath the bottom box to mark the lower limit of the samples. The GPR unit was placed directly on the ore sample for data acquisition. Figure 4

Figure 4. A stack of two boxes showing the aluminium base with the antenna positioned for acquisition.

shows a stack of two boxes with the aluminium sheet beneath and the antenna positioned for data acquisition.

Each of the three boxes for each of the sample sizes were weighed to determine the bulk density of the material (see Table I). The <25mm samples are composed of material ranging from fine, sandy material up to small gravel, allowing greater packing of the material, and hence it exhibits a greater bulk density than the coarse material. The <25mm material exhibited no significant compressing, even after being stacked and the boxes rotated into different orders. The height of the three box stack of <25mm material averaged 66cm.

The 25-50mm samples and 50-100mm samples are very irregular in shape, and enabled large air pockets to develop in the sample boxes. The height of the three boxes for both samples, rotated in a similar manner to the other sample, averaged 75cm. The surface of the rocks was irregular, however as seen in Fig. 4, the antenna was maintained parallel to the aluminium sheet.

A large, solid fragment was separated from the original ore sample from the mine. This solid fragment had dimensions of about 600mm x 300mm x 600mm (length x width x depth). The surface of the rock was somewhat irregular, with the antenna maintained parallel to the aluminium sheet during data capture.

The bulk density of the solid ore in-situ at the mine site was communicated in a private telephone conversation between the authors and a company mine geologist as 2500 kg/t, hence there are no values in Table I for the average mass and volume of the solid samples. The authors conducted small-scale experiments on the bulk density of the ore and determined the bulk density to be 2680 kg/m^3, however given that the samples were less than 2kg, it was considered the mine value was more likely to be more representative of the average rock from the mine.

The fractured ore volume within the buckets contains a mixture of air and ore fragments. As the fragment size increases, the amount of air in the volume mix will reduce, thereby approaching the bulk density of the solid ore at 2500 kg/m^3. As the fragment size reduces down to 25-50mm, initially the bulk density decreases to about half that of the solid ore as a large percentage of the volume is occupied by air. However, as the fragment size continues to reduce to <25mm, the bulk density increases again as the particle size excludes air from the mix. As Table I shows, as the bulk density of the ore samples increases, so the relative dielectric permittivity also increases.

Table I
BULK DENSITY OF SAMPLES

Sample	Avg Mass (kg)	Volume (m^3)	Bulk Density (kg/m^3)	ϵ_r
< 25mm	91.3	0.055	1660	7.0
25-50mm	78	0.063	1238	3.9
50-100mm	77.7	0.063	1222	4.1
Solid	-	-	2500	16.0

IV. RESULTS

With the samples arranged in a three-box stack, data was acquired from the stationary antenna situated on the top of the stack (see Fig. 4). Data was recorded over time, with a stationary antenna, hence, each data capture contained many traces over the same location. The data was then averaged to obtain a single trace for each sample, as shown below.

For each sample size, 6 data sets were acquired with the boxes in different orders. The processing flow was

1) Acquire data
2) Discard first and last 25% of the traces
3) Average remaining traces in the capture
4) Remove DC
5) apply dewow filter

The resulting single trace data was then manually inspected to determine the limits of the media in the scan. The initial point of amplitude was a positive peak following the surface reflection. The last point was the positive peak immediately before the aluminium sheet. Hence, the loss is attributed only to the media, and not the surface bounce or the effect of the aluminium.

The GPR equipment used for the experiments was a broadband CSIRO SiroPulseII system, using a 1.4GHz antenna. Following the same processing flow as above, the antenna response was recorded with a peak frequency of 1.43GHz and a centroid frequency of 1.44GHz. Offline processing was completed using MatGPR [18].

The centroid frequency was calculated over the range 0-3.6GHz, as it was noted that there was minimal energy above

Table II
FREQUENCY DOWNSHIFT OF SAMPLES

Sample	Height (mm)	samples	Centroid Frequency
<25mm	660	190	1.13GHz
25-50mm	750	192	1.20GHz
50-100mm	750	187	1.22GHz
Solid	600	198	0.76GHz

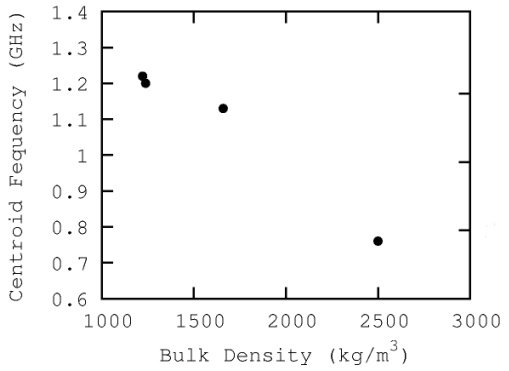

Figure 5. Graph showing relationship between bulk density and frequency centroid downshift.

this range. Table II shows the centroid frequency of the recorded data for each of the ore samples, and the average number of trace samples recorded through the media. There was no significant difference between the low bulk density <25mm, 25-50mm and 50-100mm samples. There was, however, a significant difference between the higher bulk density sample (solid) and the lower bulk density samples (<25mm, 25-50mm, 50-100mm).

Figure 5 graphs the centroid frequency (left axis) against the bulk density of the samples, showing an apparent linear relationship between frequency downshift as bulk density increases.

The relationship between bulk density and centroid frequency suggest that it is possible to determine the presence of large fragments in the draw point by determining the rate of frequency downshift over a window in the GPR trace. Given a window in time/sample length that was as large as the fragments being sought - in this case 1m or larger in depth - if the downshift approaches that of the solid ore, it may indicate the presence of a large fragment.

The results show that for a depth of about 600mm, we can detect the difference between fragmented material and solid material. This, in turn, allows us to draw a conclusion about the rock pile to that depth that would indicate the presence of a large fragment or smaller rubble. With this knowledge, the autonomous vehicle would be able to advise the system of the presence of a large fragment. The system could then close the draw point to await secondary breakage as outlined in Section I.

Given the sizes of the fractured rock fragments, scattering could be expected to affect the results. The wavelength of the transmitted signal varies from about 75mm to 150mm depending on the sample dielectric permittivity. The fragment sizes of the 50-100mm approach the wavelength of the signal, however, the difference between the 25-50mm and 50-100mm samples which have a similar bulk density but different fragment sizes, suggest that scattering may not have a significant effect. More research is required to determine the effect of scattering on the methods outlined in this paper.

Further work will be conducted to extend the depth to 2m, allowing detection of large rocks beneath a surface consisting of smaller fragmented rocks. This will also require additional testing of large fragments overborne with smaller fragments.

V. CONCLUSION

Detecting fragments that are too large for crusher units in underground mines is important to ensure the mine is able to achieve maximum efficiency in its operations. Early detection can prevent unnecessary vehicle movements, and enable coordination of manual breakage at multiple draw points by closing down sections of the mine in a controlled manner. This is essential for efficient operation of autonomous vehicles.

While improvements to GPR resolution and removing clutter to aid image interpretation are important, they suffer inherent problems whereby the earth material naturally filters high frequency components of the signal. They also require multiple A-scans or a complete B-scan to achieve sufficient information to determine fragment sizes.

This paper has shown that a relationship between signal attenuation, as observed through centroid frequency downshift, and bulk density exists. Using signal attenuation as presented in this paper provides a fast method of determining the bulk density of complex and irregular structures under illumination.

The Centroid Frequency Downshift Method is useful in this application of subsurface radar as the attenuation from the ore is high enough to cause noticeable losses of high frequencies during propagation, indicating an increase in material dielectric properties. The results show this would assist in determining the presence of large rocks with minimal data collection at the draw point of an underground mine.

ACKNOWLEDGMENT

The Authors would like to thank Newcrest Mining Ltd (www.newcrest.com.au) for funding the work presented here, and Mr Chris Lewis of the CSIRO (www.csiro.au) for his

assistance with GPR equipment. The Authors are also appreciative of the comments given by the reviewers to improve the presentation of the research outcomes.

REFERENCES

[1] P. Ridley and P. Corke, "Autonomous control of an underground mining vehicle," in *Australian Conference on Robotics and Automation*, 2001, pp. 26–31.

[2] P. Corke, J. Roberts, J. Cunningham, and D. Hainsworth, *Mining Robotics*, 1st ed., ser. Handbook of Robotics. Springer, 2008, ch. 49, pp. 1127–1150.

[3] N. Maerz, "Technical and computational aspects of the measurement of aggregate shape by digital image analysis," *Journal of Computing in Civil Engineering*, vol. 18, no. 1, pp. 10–18, January 2004.

[4] L. Conyers, *Ground Penetrating Radar for Archaeology*. Alta Mira Press, 2004.

[5] Y.-L. Chen and J. J. Chow, "Ground penetrating radar signal processing improves mapping accuracy of underground voids and seawater table; an application in deteriorating coastal structure, nanfangao port, taiwan," *Environmental Geology*, vol. 53, pp. 445–455, 2007.

[6] W. Lai, T. Kind, and H. Wiggenhauser, "Using ground penetrating radar and time-frequency analysis to characterize construction materials," *NDT and E International*, vol. 44, pp. 111–120, 2011.

[7] C. Rappaport, M. El-Shenawee, and H. Zhan, "Suppressing GPR clutter from randomly rough ground surfaces to enhance nonmetallic mine detection," *Subsurface Sensing Technologies and Applications*, vol. 4, no. 4, pp. 311–326, 2003.

[8] A. Benter, W. Moore, and R. Xu, "Reducing clutter from ground penetrating radar images of rock piles," in *Australian Mining Technology Conference*. CRC Mining, 2009.

[9] R. Mardeni, R. S. A. R. Abdullah, and H. Z. M. Shafri, "Road pavement density analysis using a new non-destructive ground penetrating radar system," *Progress in Electromagnetic Research B*, vol. 21, pp. 399–417, 2010.

[10] D. Ranalli, M. Scozzafava, M. Tallini, and S. Colagrande, "GPR signal attenuation vs. depth on damaged flexible road pavement," in *Advanced Ground Penetrating Radar, 2007, 4th International Workshop on*, 2007, pp. 300–305.

[11] R. Roberts, I. Al-Qadi, J. Tutumluer, E. Boyle, and T. Sussmann, "Advances in railroad ballast evaluation using 2GHz horn antennas," *Proceedings of the 11th International Conference in Ground Penetrating Radar*, 2006.

[12] P. Neto and W. Medeiros, "A Practical Approach to Correct Attenuation Effects in GPR Data," *Journal of Applied Geophysics*, vol. 59, pp. 140–151, 2006.

[13] A. Benedetto, "Water Content Evaluation in Unsaturated Soil Using GPR Signal Analysis in the Frequency Domain," *Journal of Applied Geophysics*, no. 71, pp. 26–35, 2010.

[14] G. Turner and A. Siggins, "Constant Q Attenuation of Subsurface Radar Pulses," *Geophysics*, vol. 59, no. 8, pp. 1192–1200, 1994.

[15] L. Liu, J. Lane, and Y. Quan, "Radar attenuation tomography using centroid frequency downshift method," *Journal of Applied Geophysics*, vol. 40, pp. 105–116, 1998.

[16] G. R. Olhoeft, "Electrical, magnetic, and geometric properties that determine ground penetrating radar performance," in *Proceedings of GPR98, Seventh Intl Conference on Ground Penetrating Radar, Lawrence,USA*, 1998.

[17] L. Zhang, S. Liu, and J. Wu, "Layered media Q estimation for GPR signal processing using the frequency shift method," in *Proceedings of 2010 International Conference on Computer Application and System Modeling*, 2010.

[18] A. Tzanis, "Matgpr: A freeware matlab package for the analysis of common-offset GPR data," *Geophysical Research Abstracts*, vol. 8, no. 09448, 2006.